JOURNAL OF AIRCRAFT
Vol. 50, No. 3, May–June 2013

Simultaneous Helicopter and Control-System Design

Tugrul Oktay*
Erciyes University, 38039 Kayseri, Turkey
and
Cornel Sultan†
Virginia Polytechnic Institute and State University, Blacksburg, Virginia 24061

DOI: 10.2514/1.C032043

This article proposes simultaneous helicopter and control system design and illustrates its advantages. First, the traditional, sequential approach in which a satisfactory control system is designed for a given helicopter is applied. Then, a novel approach, in which the helicopter and control system are simultaneously designed, is applied to redesign the entire system. This redesign process involves selecting certain helicopter parameters as well as control system parameters. For both design procedures the key objectives are to minimize control energy and satisfy prescribed variance constraints on specific outputs. In order to solve the complex optimization problem corresponding to the simultaneous design approach, an efficient solution algorithm is developed by modifying the simultaneous perturbation stochastic approximation method to account for limits on optimization parameters. The algorithm is applied to redesign helicopters using models generated in straight level as well as maneuvering flight conditions. The performance of the designs obtained using the sequential and simultaneous design approaches is compared and the redesign process is thoroughly investigated. Finally, the robustness of the redesigned systems is also studied.

Nomenclature

c	=	blade chord length, m
K_β	=	blade flapping-spring stiffness coefficient, $\mathrm{N \cdot m/rad}$
m	=	blade linear mass density, kg/m
p, q, r	=	helicopter angular velocities, rad/s
R	=	blade length, m
u, v, w	=	helicopter linear velocities, m/s
V_A	=	flight speed of helicopter, m/s
γ_{FP}	=	flight-path angle, rad
$\beta_0, \beta_c, \beta_s, \beta_d$	=	collective, two cyclic, and differential blade flapping angles, rad
$\zeta_0, \zeta_c, \zeta_s, \zeta_d$	=	collective, two cyclic, and differential blade lagging angles, rad
θ_T	=	collective tail rotor angle, rad
θ_{tw}	=	blade twist, rad
$\theta_0, \theta_c, \theta_s$	=	collective and two cyclic blade pitch angles, rad
ϕ_A, θ_A, ψ_A	=	helicopter Euler angles, rad
$\dot{\psi}_A$	=	helicopter turn rate, rad/s
Ω	=	main-rotor angular speed, rad/s

I. Introduction

TRADITIONALLY, a model of the system to be controlled (e.g., helicopter, structure, etc.), also referred to as the "plant" in the following, is given a priori to the control engineer who has no influence on this system's design. However, it is known that the plant and control-system design problems are not independent [1,2]. Changes in some plant parameters may improve performance significantly, as shown for example in [3–5]. The traditional sequential approach: 1) design the plant first, and 2) design the control system after that does not provide the best overall design [1,2]. Ideally, we should simultaneously design the system to be controlled as well as the control system such that a given objective (e.g., cost function) is optimized, eventually subject to additional constraints. In this article we pursue this idea and redesign a helicopter by simultaneously designing the helicopter over blade and operation parameters and a control system to minimize the active control energy while obeying constraints on the physical parameters of the helicopter and on the closed-loop system response.

Previous work in helicopter redesign was focused on passive design (i.e., control-system parameters were not included). For example, in [6], a redesign optimization study is performed in which rotor dynamics and flight dynamics are simultaneously taken into account to maximize the damping of a rotor lag mode with respect to certain design parameters (e.g., blade torsion stiffness, blade chord length). In another study [7], vibratory loads at the rotor hub, which are the main sources of helicopter vibration, are reduced by redesigning the helicopter using certain variables (e.g., blade lag and torsion stiffness). Several other papers [8,9] also report helicopter redesign studies, while in [3,4] the main-rotor speed is allowed to vary to improve helicopter's stability.

In the simultaneous design study presented in this article we use complex helicopter models that include relevant physics, such as an analytical formulation for fuselage aerodynamics, blade flapping and lead lagging, tail rotor and empennage aerodynamics, main-rotor downwash, landing gear effects, etc. The main philosophy of our modeling process is to develop physics-based, control-oriented models that capture the "essential dynamics". By essential dynamics, we mean (in addition to the dynamics to be controlled) dynamics directly affected by control design and crucial for safe and performant operation. For example, even if the primary goal of the control design is to control flight dynamics modes, we are interested to capture blade flapping and lead-lagging modes and monitor their behavior in the closed-loop configuration. Of course, development of such models requires a multibody dynamics approach, presented in detail in [10], which also shows how these models have been validated against trim and dynamics data that are available in the published literature.

For control design, the models discussed in the previous paragraph are linearized around specific flight conditions (i.e., straight level flight, level banked turn, and helical turn). The modern controllers we study are variance-constrained controllers that present several advantages. First, these controllers are enhanced linear quadratic Gaussian (LQG) controllers that use state estimators (i.e., Kalman filters). State estimators are crucial for complex systems such as helicopters because some states cannot be easily measured. Second, these controllers use second-order information, namely the state covariance matrix [11–19]. This is very important for multivariable

Received 16 July 2012; revision received 8 October 2012; accepted for publication 20 October 2012; published online 25 February 2013.

*Assistant Professor, Civil Aviation School.
†Assistant Professor, Department of Aerospace and Ocean Engineering. Senior Member AIAA.

control design because it enables parameterization of all stabilizing controllers in terms of the state covariance matrix, which is physically meaningful. Third, for strongly coupled, large multi-input multi-output systems, like the ones encountered in helicopter control and particularly in our work [10], variance constrained control design methods guarantee good transient behavior of individual variables by enforcing upper bounds on the variance of these variables.

The helicopter design parameters involved in this study are blade length, chord length, flapping-spring stiffness, twist, linear mass density, and main-rotor angular speed. Selection of these particular parameters as design variables is primarily motivated by technological advances. Specifically, it has been very recently indicated that it is both feasible and desirable to alter the blade length, blade chord length, blade flapping-spring stiffness, blade twist, blade linear mass density, and main-rotor angular speed to improve the handling qualities and performance of helicopters; see [3–5,20–26]. For example, in [5], several morphing concepts (i.e., variable main-rotor angular speed, blade length, blade chord length, and blade twist) are investigated to improve helicopter performance, showing that both variable rotor speed and variable blade chord lead to significant improvement in the rotor performance in cruise. Moreover, in [26], a morphing mechanism to extend the chord of a section of the helicopter rotor blade is presented. In this study, a morphing cellular structure is developed, and the blade chord is increased by 30%. This mechanism is first computationally designed, then also fabricated and experimentally proven to be reliable and effective. This article intends to exploit and promote these very recent technological advances in the area of morphing helicopter blade by showing how, when combined with advanced control design, they can substantially improve helicopter performance.

The simultaneous design problem we obtain by combining our helicopter models and dynamic feedback variance controllers is a very complex constrained optimization problem, which does not allow analytical computation of derivatives (e.g., gradients, Hessians). Because deterministic numerical approximation of these derivatives for such complex problems is prohibitive and possibly numerically unstable, we selected a fast stochastic optimization method, simultaneous perturbation stochastic approximation (SPSA), to solve the optimization problem. SPSA was selected primarily due to its previous success in rapidly solving similar, highly complex and constrained optimization problems [27,28] and due to existing theoretical guarantees on its convergence in probability to an optimal solution [27]. Moreover, in this paper, we improved the classical SPSA by taking into account inequality constraints on the design parameters. This resulted in an algorithm that is very efficient in rapidly decreasing the control energy while satisfying all the constraints, illustrating the effectiveness of using SPSA for simultaneous helicopter and control-system design. We also comprehensively evaluated the redesigned helicopters obtained using our design method. For this purpose, complex helicopter models were linearized around different straight level flight conditions as well as maneuvering-flight conditions. Then, their performance, including control energy savings and closed-loop responses, were compared with those of the nominal helicopter. Robustness properties of these redesigned helicopters were also investigated with respect to modeling uncertainties (i.e., flight conditions and helicopter inertial parameters variations), leading to the evaluation of controllers that are aware and unaware of the flight condition.

This article is an extended and enriched version of our AIAA conference paper Ref. [29], which only included the main redesign idea and simple examples, without comprehensive evaluation or robustness studies. The main contributions of this article are a complete process of simultaneous helicopter and advanced control-system design, including a thorough analysis of robustness properties of the redesigned helicopters with respect to modeling uncertainties. This is the first article which shows that such a process is feasible and effective, resulting in substantial energy savings (from 33 to 57%) with small changes in design parameters (from 5 to 10%) over a wide flight envelope. Evidence is provided to show that the simultaneous design approach is clearly superior in terms of achievable performance with respect to the classical sequential approach. A novel, adaptive SPSA algorithm, which accounts for upper and lower limits on optimization parameters, is also developed, and its performance is evaluated.

II. Model and Control System

A. Control-Oriented Helicopter Model

Our modeling approach, presented in detail in [10] (see also [29,30]), involves application of physics principles, directly leading to dynamic models composed of finite sets of ordinary differential equations (ODEs). These models are extremely advantageous for control-system design because they facilitate the direct use of modern control theory. Modern control design relies on state-space representations of the system's dynamics, which are readily obtained from ODEs. In contrast, if application of the physics principles leads to partial differential equations (PDEs) models, to obtain a finite set of ODEs from the infinite dimensional set of PDEs, much work is required to retain a finite number of modes. In this case, only several ODEs are retained, usually selected to capture the modes that are considered relevant for control-system design. This process results in qualitative and quantitative alteration of the original PDEs based mathematical model and complicates the verification and validation of the control system. On the other hand, the models obtained using our approach consist of nonlinear ODEs but have too many terms, making their use in fast computation impossible. Therefore, a systematic simplification method presented in detail in [10], called "ordering scheme," was applied to reduce the number of terms.

The helicopter model obtained using the philosophy summarized previously includes fuselage, empennage, landing gear, fully articulated main rotor (i.e., with four blades), main-rotor downwash, and tail rotor [10]. As a consequence, the model is fairly complex with a total of 29 equations: 9 fuselage equations, 16 blade flapping and lead-lagging equations, 3 static main-rotor downwash equations, and an additional flight-path angle algebraic equation. For this study, we considered several flight conditions: straight level flight, level banked turn, and helical turn, briefly described next. For these turning flights we obtained 21 trim equations (i.e., $0 = 0$ equations are eliminated) with 21 unknowns, which were solved using Matlab.

Level banked turn is a planar (i.e., two-dimensional), circular maneuver in which the helicopter banks toward the center of the turning circle (see Fig. 1a). For helicopters, the aircraft roll angle ϕ_A is, in general, slightly different from the bank angle ϕ_B. Coordinated banked turn is a banked turn with $\phi_A = \phi_B$, but this is not the focus of this work. Figure 1a depicts these angles for a particular case ($\theta_A = 0$), with $F_{\text{resultant}}$ representing the sum of the gravitational (W) and centrifugal (F_{cf}) forces. Helical turn is a spatial (i.e., three-dimensional) maneuver in which the helicopter moves along a helix with constant speed (see Fig. 1b). Note that $\dot{\psi}_A > 0$ is a clockwise turn, and $\dot{\psi}_A < 0$ is a counterclockwise turn (viewed from the top), while $\gamma_{\text{FP}} > 0$ means that the flight is ascending and $\gamma_{\text{FP}} < 0$ means that it is descending [10,29,30].

After trimming, the model was linearized around the particular trim condition using Maple, yielding a continuous linear time-invariant (LTI) system (i.e., the plant):

$$\dot{x}_p = A_p x_p + B_p u \tag{1}$$

where x_p and u are the perturbed states and controls. Matrices A_p and B_p are of size 25×25 and 25×4. There are 25 states (nine fuselage states, eight blade flapping states, and eight blade lead-lagging states), 3 main rotor (collective and two cyclic blade pitch angles), and 1 tail rotor (collective angle) control inputs. A Puma SA 330 helicopter (see [31]) was used to validate the models used in this article [10].

B. Output Variance Constrained Control

For control design, we selected output variance constrained (OVC) controllers, which are dynamic feedback controllers that minimize control energy subject to variance constraints on the outputs. The feasibility of using these controllers for our complex,

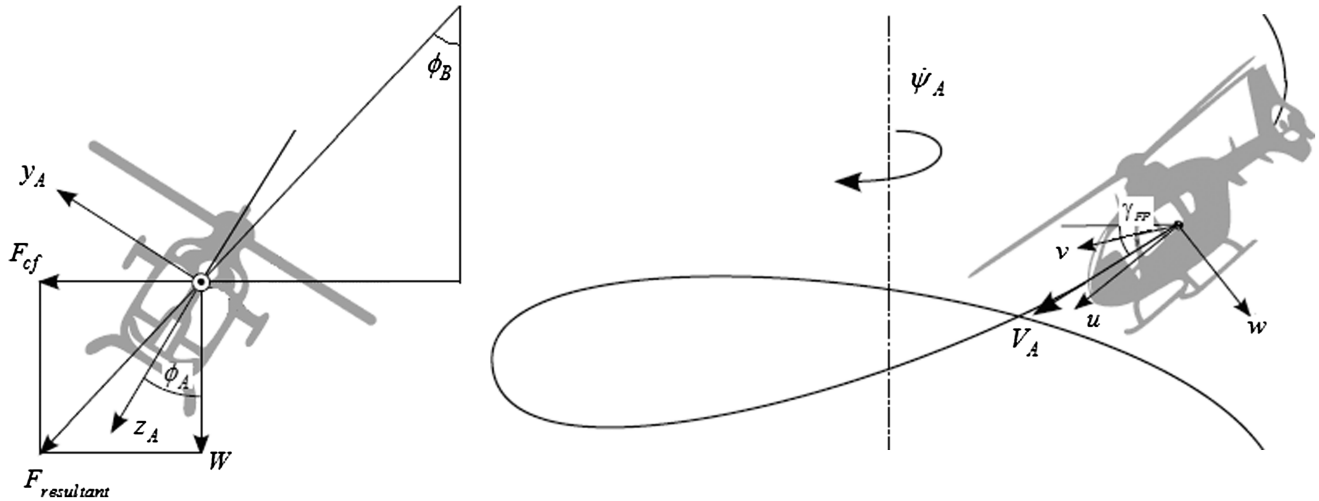

a) Level banked turn **b) Helical turn**

Fig. 1 Two types of turns: a) level banked, and b) helical.

control-oriented helicopter models was illustrated recently in [19]. For OVC design, the problem described next must be solved [11–19].

Given a continuous LTI, stabilizable and detectable system (i.e., the plant),

$$\dot{x}_p = A_p x_p + B_p u + w_p, \qquad y = C_p x_p, \qquad z = M_p x_p + v \tag{2}$$

and a positive–definite input penalty $R > 0$, find a full-order dynamic controller,

$$\dot{x}_c = A_c x_c + F z, \qquad u = G x_c \tag{3}$$

to solve the problem

$$\min_{A_c,F,G} J = E_\infty u^T R u = \mathrm{tr}(RG\aleph G^T) \tag{4}$$

subject to

$$E_\infty y_i^2 \le \sigma_i^2, \qquad i = 1, \ldots, n_y \tag{5}$$

Here, y is the vector of system outputs, z represents sensor measurements, w_p and v are zero-mean uncorrelated process and measurement Gaussian white noises with intensities W_p and V, respectively, and x_c is the controller state vector. Matrices F and G are state estimator and controller gain, respectively; J is the control energy; $\aleph$ is the state covariance matrix; σ_i^2 is the upper bound imposed on the ith output variance; and n_y is the number of outputs. Last, tr denotes the matrix trace operator, min is the minimization operator, $E_\infty \triangleq \lim_{t\to\infty} E$, and E is the expectation operator.

Effectively, OVCs are enhanced LQGs because they guarantee satisfaction of constraints of output variances. The OVC solution actually reduces to a LQG problem solution by choosing output penalty $Q > 0$ depending on the inequality constraints. An algorithm for the selection of Q is presented in [14,15]. After converging on Q, OVC parameters are

$$\begin{aligned} A_c &= A_p + B_p G - F M_p, \qquad F = X M_p^T V^{-1}, \\ G &= -R^{-1} B_p^T K \end{aligned} \tag{6}$$

where X and K are solutions of two algebraic Riccati equations:

$$\begin{aligned} 0 &= X A_p^T + A_p X - X M_p^T V^{-1} M_p X + W_p, \\ 0 &= K A_p + A_p^T K - K B_p R^{-1} B_p^T K + C_p^T Q C_p \end{aligned} \tag{7}$$

Compared to standard LQG, where Q and R are selected ad hoc and constraints are not taken into account, OVC provides an intelligent way of choosing Q, which guarantees satisfaction of constraints on the variance of the outputs while minimizing control energy.

Note that, for all of the numerical experiments reported herein (i.e., OVC designs and closed-loop simulations), the sensor measurements were helicopter linear velocities, angular velocities, and Euler angles. The outputs of interest were helicopter Euler angles.

III. Statement of the Design Problem

The simultaneous helicopter and control-system design problem is summarized next:

$$\min_{A_c,F,G,x} J = E_\infty u^T R u \tag{8}$$

subject to Eqs. (2, 3, 5) where $x = \{c, K_\beta, m, R, \theta_{\mathrm{tw}}, \Omega\}$ is the set of helicopter optimization parameters. The elements of x are constrained, i.e., $x_{i_{\min}} \le x_i \le x_{i_{\max}}$ (see Table 1).

Note that matrices A_p and B_p are functions of x. This leads to a complicated optimization problem in which both the objective J and the variance constraints depend on the optimization variables in a sophisticated manner; the expectation operator has to be applied to time-varying responses that depend on x as well as on controller parameters (i.e., A_c, F, G), leading to a very difficult optimization problem, whose solution is discussed next.

IV. Simultaneous Perturbation Stochastic Approximation

Because of the intricate dependency of J and the variance constraints on the optimization variables, computation of their derivatives with respect to these variables is impossible analytically. This recommends the application of certain stochastic optimization techniques. Specifically, in this article, simultaneous perturbation stochastic approximation (SPSA) [27], which has proven effective in solving other complex problems [28], including optimization of nondifferentiable functions [32], has been selected to solve the

Table 1 Design variables and constraints

Design variable	Nominal value	Lower bound $\Delta x_i/x_i$	Upper bound $\Delta x_i/x_i$
c	0.5401 m	−0.05	0.05
K_β	48, 149 N · m/rad	−0.05	0.05
m	9.1 kg/m	−0.05	0.05
R	7.5 m	−0.05	0.05
θ_{tw}	−0.14 rad	−0.05	0.05
Ω	27 rad/s	−0.05	0.05

problem described in the previous section. SPSA has many advantages. For example, SPSA uses only two evaluations of the objective for the computation of the gradient [27]. Also, numerical experiments indicated that SPSA is more efficient in solving many optimization problems compared to other computationally expensive algorithms like genetic algorithms and fast simulated annealing [33]. Moreover, SPSA was also successful in solving constrained optimization problems [34]. Finally, under certain conditions (see [27]) strong convergence of SPSA has been theoretically proved. One issue with theoretical guarantees for SPSA convergence is that the key conditions (e.g., that the objective function must be three times continuously differentiable and the third derivatives uniformly bounded) are difficult to verify. Therefore, because in most practical applications the objective is complicated and its derivatives are not easily available, one directly applies the SPSA algorithm and monitors its behavior. Another feature of SPSA is the inherent randomness due to its stochastic nature. This issue is very easily resolved by running SPSA several times and selecting the best solution.

In this study, a modified version of the classical SPSA, which accounts for upper and lower limit constraints on optimization parameters, is developed as discussed next.

A. Simultaneous Perturbation Stochastic Approximation Formulation

Let x denote the vector of optimization variables. In classical SPSA, if $x_{[k]}$ is the estimate of x at the kth iteration, then

$$x_{[k+1]} = x_{[k]} - a_k g_{[k]} \tag{9}$$

where a_k is a decreasing sequence of positive numbers, and $g_{[k]}$ is the estimate of the objective's gradient at $x_{[k]}$, computed using a simultaneous perturbation as follows. Let $\Delta_{[k]} \in R^p$ be a vector of p mutually independent mean-zero random variables $\{\Delta_{[k]1} \quad \Delta_{[k]2} \quad \ldots \Delta_{[k]p}\}$ satisfying certain conditions [32,35]. Then $g_{[k]}$ is

$$g_{[k]} = \left[\frac{\Gamma_+ - \Gamma_-}{2d_k\Delta_{[k]1}} \cdots \frac{\Gamma_+ - \Gamma_-}{2d_k\Delta_{[k]p}}\right]^T \tag{10}$$

where Γ_+ and Γ_- are estimates of the objective evaluated at $x_{[k]} + d_k\Delta_{[k]}$ and $x_{[k]} - d_k\Delta_{[k]}$, respectively.

In this article a novel adaptive SPSA that accounts for the constraints that optimization variables must be between lower and upper limits (i.e., $x_{i_{\min}} \le x_i \le x_{i_{\max}}$) is developed to solve related problems. All the perturbed vector elements, $x_{[k]} + d_k\Delta_{[k]}$ and $x_{[k]} - d_k\Delta_{[k]}$, are also required to be between the prescribed lower and upper limits. Using these requirements and the guidelines provided in [27] for the selection of sequences a_k and d_k, we chose d_k as (see [10], pages 187–188 for details)

$$d_k = \min\left\{d/k^{\Theta}, 0.95\min_i\{\min\{\eta_{l_i}\}, \min\{\eta_{u_i}\}\}\right\} \tag{11}$$

Here, η_l and η_u are vectors whose components are $(x_{[k]i} - x_{\min_i})/\Delta_{[k]i}$ for each positive $\Delta_{[k]i}$ and $(x_{\max_i} - x_{[k]i})/\Delta_{[k]i}$ for each negative $\Delta_{[k]i}$, respectively. Likewise, we selected a_k as

$$a_k = \min\left\{a/(S+k)^{\lambda}, 0.95\min_i\{\min(\mu_{i_l}), \min(\mu_{i_u})\}\right\} \tag{12}$$

where μ_l and μ_u are vectors whose components are $(x_{[k]i} - x_{\min_i})/g_{[k]i}$ for each positive $g_{[k]i}$ and $(x_{[k]i} - x_{\max_i})/g_{[k]i}$ for each negative $g_{[k]i}$, respectively. The other SPSA parameters d, a, λ, Θ, S are chosen using guidelines provided in [27,36–38].

B. Solution Algorithm

We are now prepared to describe the algorithm used to solve the simultaneous helicopter and control-system design problem of Sec. III.

Step 1: Set $k = 1$ and choose initial values for the optimization parameters, $x = x_{[k]}$, and a specific flight condition (e.g., $V_A =$ 40 kt straight level flight).

Step 2: Compute A_p and B_p, design the corresponding OVC using Eqs. (6 and 7), and obtain the current value of the objective Γ_k using Eq. (8); note that $\Gamma_k = J_k$ for OVC.

Step 3: Perturb $x_{[k]}$ to $x_{[k]} + d_k\Delta_{[k]}$ and $x_{[k]} - d_k\Delta_{[k]}$ and solve the corresponding OVC problems to obtain Γ_+ and Γ_-, respectively. Then compute the approximate gradient, $g_{[k]}$, using Eq. (10) with d_k given by Eq. (11).

Step 4: If $\|a_k g_{[k]}\| < \delta x$, where a_k is given by Eq. (12) and δx is the minimum allowed variation of x, or $k+1$ is greater than the maximum number of iterations allowed, exit, else calculate the next estimate of x, $x_{[k+1]}$, using Eq. (9), set $k = k+1$, and return to step 2.

V. Results

A. Simultaneous Perturbation Stochastic Approximation Results

To investigate the performance of the previous algorithm on simultaneous helicopter and control-system design, we first linearized our model for $V_A = 40$ kt (20.58 m/s), $\gamma_{\mathrm{FP}} = 0$ rad, $\dot{\psi}_A =$ 0 rad/s (straight level flight). We then designed the corresponding OVC for this linearized model. We shall further refer to this design (i.e., the helicopter and the corresponding OVC) as "the nominal system" (note that all the scenarios examined in this paper are summarized in Table A.1). Clearly, this corresponds to the traditional, sequential design approach. Next, we applied the algorithm (see Sec. IV.B) to redesign the helicopter and the control system using nominal values of helicopter parameters as initial conditions. The resulting design will be referred to as "the redesigned system". For all of the OVCs designed, we considered $\sigma^2 = 10^{-4}[1 \quad 1 \quad 0.1]$; recall that these are variance constraints on helicopter Euler angles [see Eq. (5)]. Small values for the output variance constraints are recommended to achieve good overall behavior of the outputs.

Using SPSA parameters, $S = 10$, $\lambda = 0.602$, $a = 100$, $d = 20$, $\Theta = 0.101$, very fast convergence of the algorithm described in Sec. IV.B was achieved (see Fig. 2). Furthermore, the control energy corresponding to the redesigned system thus obtained was 33.3% lower than the control energy of the nominal system. Table 1 summarizes the optimization parameters and their lower and upper bounds while Table 2 gives their optimum values.

We remark that the fact that the algorithm is very effective in decreasing the value of the objective J in the first several iterations (see Fig. 2) is a characteristic of SPSA, ascertained in other complex optimization problems [28]. This property of SPSA, in addition to the fact that it uses fewer computations per iteration than other optimizers [27], makes SPSA very attractive as a fast optimizer.

B. Evaluation of the Redesign Process for Energy Saving

To further evaluate the performance of the redesigned helicopter, we linearized this helicopter's model around different straight level flight conditions, i.e., between $V_A = 1$ kt (0.5145 m/s) to 80 kts (41.1565 m/s). Then, at each flight condition, we designed the corresponding OVC and computed its cost J_r. At the same flight conditions, we also linearized the nominal helicopter (which corresponds to the nominal design), designed the corresponding OVCs, and computed the cost J_n. We then computed the relative variation of

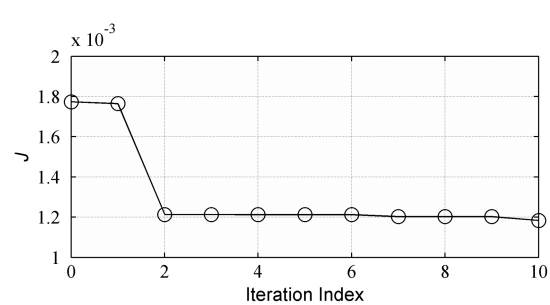

Fig. 2 Control energy optimization using SPSA.

Table 2 Optimum design variables

Design variable	Optimum value	Change $\Delta x_i/x_i$
c	0.5662 m	0.04840
K_β	50, 543.4498 N · m/rad	0.04973
m	9.5400 kg/m	0.04835
R	7.1258 m	−0.04990
θ_{tw}	−0.1470 rad	0.04969
Ω	25.6527 rad/s	−0.04990

the cost as $\%J = 100(J_n - J_r)/J_n$ for each flight condition. Figure 3 shows the variation of $\%J$ with respect to V_A. It is clear from Fig. 3 that, using the redesigned helicopter, considerable control energy is saved for each flight condition. This is advantageous in practice because it shows that, even though we optimized the design at a single, particular flight condition, the helicopter obtained that way has better performance than the nominal one across a wide flight envelope.

Furthermore, we repeated the previous scenario for helical turns. Specifically, we first considered the nominal helicopter, we assumed that the helicopter velocity takes values between $V_A = 1$ kt to 80 kts and we computed the trim solutions for helical turns characterized by V_A, $\gamma_{FP} = 0.1$ rad and $\dot{\psi}_A = 0.1$ rad/s. For each of these flight conditions, we linearized the nominal helicopter model, designed the corresponding OVCs, and computed the cost J. We then performed the same study using, instead of the nominal helicopter, the redesigned one. In the end, we reached a similar conclusion: substantial energy savings (around 30%) are obtained using the redesigned helicopter.

To further convince ourselves of the advantages of simultaneous helicopter and control-system design, we used two other flight conditions to redesign the helicopter: $V_A = 1$ kt and $V_A = 80$ kts (straight level flights). We used the same SPSA parameters as before

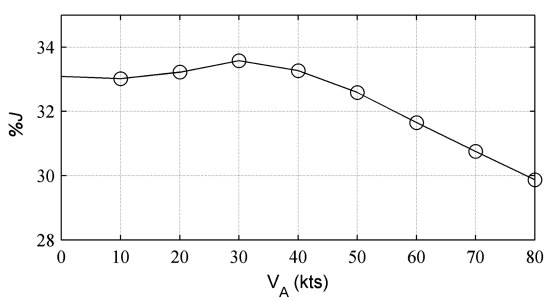

Fig. 3 Relative energy saving with respect to V_A ($\gamma_{FP} = 0$ rad, $\dot{\psi}_A = 0$ rad/s).

and obtained two different redesigned helicopters. We performed the same analysis as before and arrived at very similar conclusions: SPSA converges very fast, optimal design variables are very close to the ones in Table 2, and the behavior of $\%J$ with respect to V_A is similar to the one in Fig. 3 [10]. Ultimately, and most importantly, substantial energy savings across a wide flight envelope, which also include maneuvering flights (e.g., helical turns), are achieved. It should be emphasized that the energy savings reported herein are obtained using linearized helicopter models. In practical applications, because of inherent helicopter nonlinearities, the real energy savings can be slightly different from values computed using linearized models.

This thorough analysis indicates that it is always recommended to perform simultaneous helicopter and control-system design (i.e., the control engineer should be involved early in the design process). Even if a nominal helicopter is prescribed, substantial performance improvement in terms of control energy can be achieved with very small, tolerable changes in nominal parameters (around ±5% like in our examples). Furthermore, the previous analysis also shows that the design process presented herein is robust; we reached almost similar optimal designs and similar conclusions regarding the cost savings, even though the flight conditions we linearized about were substantially different. Therefore, implementing one design will be satisfactory for a large set of operational conditions.

C. Closed-Loop Performance Comparison

After simultaneous design, we investigated the closed-loop system performance of nominal and redesigned helicopters using the nominal system and the redesigned system described in Sec. V.A. For the discussion to follow, we shall also refer to the closed-loop system that corresponds to the nominal system as the first closed-loop system (i.e., the first closed-loop system is created using the OVC designed for the nominal helicopter and coupled to the nominal helicopter). Likewise, we shall refer to the closed-loop system that corresponds to the redesigned system as the second closed-loop system (i.e., the second closed-loop system is created using the OVC designed for the redesigned helicopter and coupled to the redesigned helicopter).

In Figs. 4–6, responses of helicopter Euler angle states, linear velocity states, and angular velocity states are given when the first closed-loop system (solid line) and second closed-loop system (dotted line) are both excited by white noise perturbations. In Figs. 7 and 8, responses of some blade flapping and lagging states (i.e., collective and two cyclics) are given for the first closed-loop system (solid line) and second closed-loop system (dotted line). Note that these states correspond to the essential dynamics captured by our models. In Fig. 9, responses of all controls are given for the first closed-loop system (solid line) and second closed-loop system (dotted line).

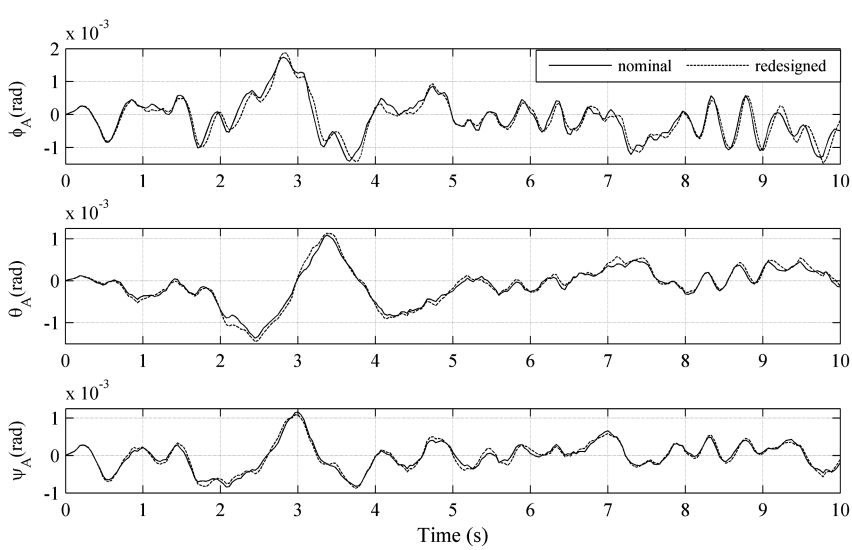

Fig. 4 Helicopter Euler angles responses before (nominal) and after redesign.

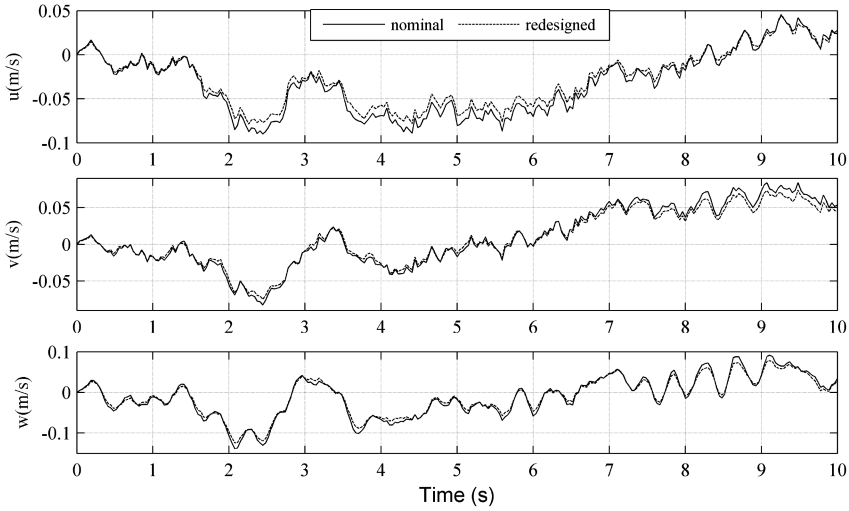

Fig. 5 Helicopter linear velocity responses before (nominal) and after redesign.

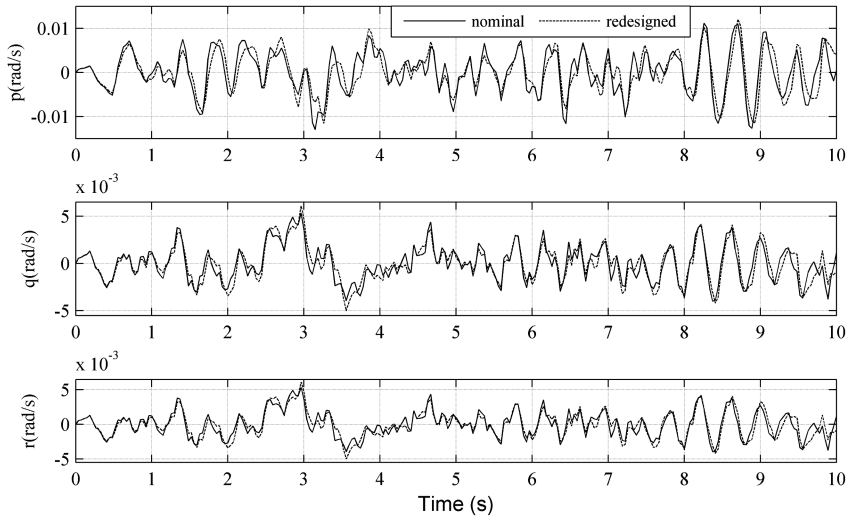

Fig. 6 Helicopter angular velocity responses before (nominal) and after redesign.

From Fig. 4, it can be seen that, before and after redesign, the qualitative (i.e., shape of the response) and quantitative (i.e., magnitude of the response) behaviors of helicopter Euler angles are practically the same. This explains the fact that the variances of outputs of interest (i.e., helicopter Euler angles) are very close and satisfy constraints [Eq. (5)]. From Figs. 5 and 6, we ascertain that the linear and angular velocity states do not experience catastrophic behavior (i.e., fast and large variations) before and after redesign and their qualitative behavior is similar. This good behavior is explained by the exponentially stabilizing effect of OVC [10].

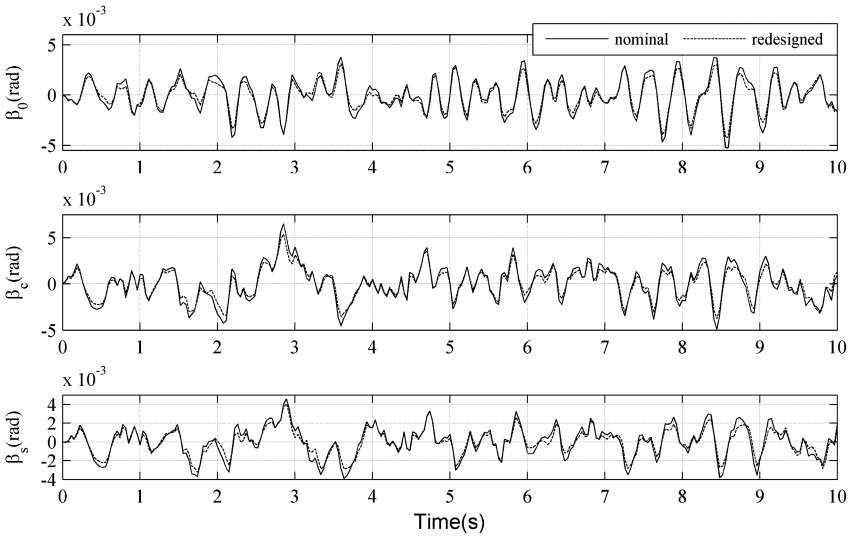

Fig. 7 Some helicopter blade flapping angles responses before (nominal) and after redesign.

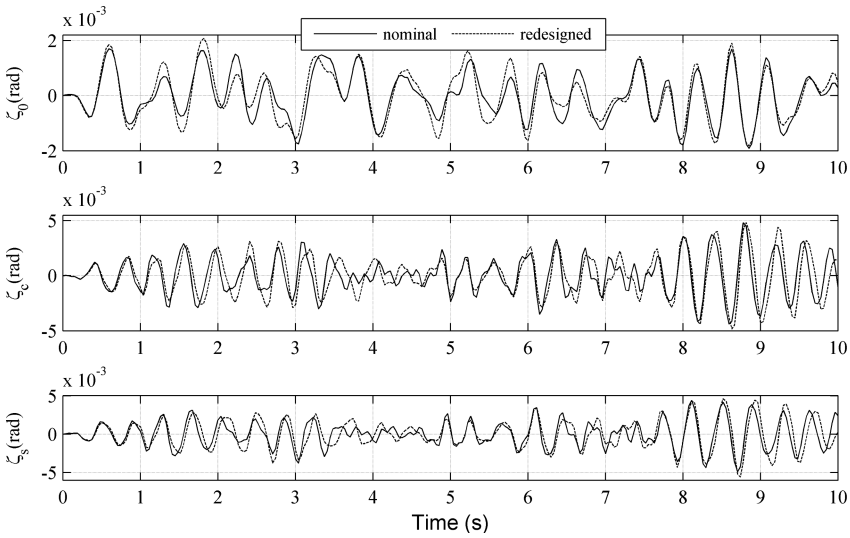

Fig. 8 Some helicopter blade lead-lagging angles responses before (nominal) and after redesign.

From Figs. 7 and 8, it can be easily concluded that blade flapping and lagging angle states (e.g., $\beta_0, \beta_c, \beta_s, \zeta_0, \zeta_c, \zeta_s$) do not experience catastrophic behavior, and their qualitative behavior is similar before and after simultaneous helicopter and control-system design. This observation is also valid for differential flapping and lagging angle states (i.e., β_d and ζ_d [10]). This good behavior is also explained by the exponentially stabilizing effect of OVC.

From Fig. 9, it can also be seen that the controls variations (i.e., θ_0, θ_c, θ_s, and θ_T) from their trim values slightly decrease after redesign (for example, peak values of solid lines are smaller than those of dotted lines), which explains the considerable reduction of control energy. This result can be seen better in Fig. 10 (zoom for θ_0, θ_c, and θ_s).

Note that all of the responses plotted in Figs. 4–19 are deviations from trim values in this article.

D. Robustness of the Redesigned System

For any engineering design, robustness is a key requirement that guarantees that the system has the capability to operate properly in the presence of uncertainties. Therefore, we also thoroughly investigated closed-loop stability robustness properties of the redesigned helicopter. The reader should also be reminded that OVC controllers are LQG-based controllers, and LQGs do not have guaranteed stability margins. Therefore, we focus on the robustness analysis of designed OVCs in this article. For this purpose, the following scenarios were considered.

1) The OVC controller designed for the nominal flight condition (i.e., straight level flight at $V_A = 40$ kts) is used for a different flight condition (i.e., helical turn with $V_A = 80$ kts, $\gamma_{\mathrm{FP}} = 0.1$ rad, and $\dot{\psi}_A = 0.1$ rad/s, etc.). The key question is, "Does this controller stabilize flight conditions that are different from the nominal one?"

2) A controller designed for an "inertially certain" model (i.e., a model for which there are *no* variations in helicopter inertial parameters) is used at the same flight condition on the same type of model but which experiences uncertainties in *all* helicopter inertial parameters (helicopter mass and helicopter inertia matrix elements). The key question is, "Are the corresponding closed-loop systems stable for these modeling uncertainties?"

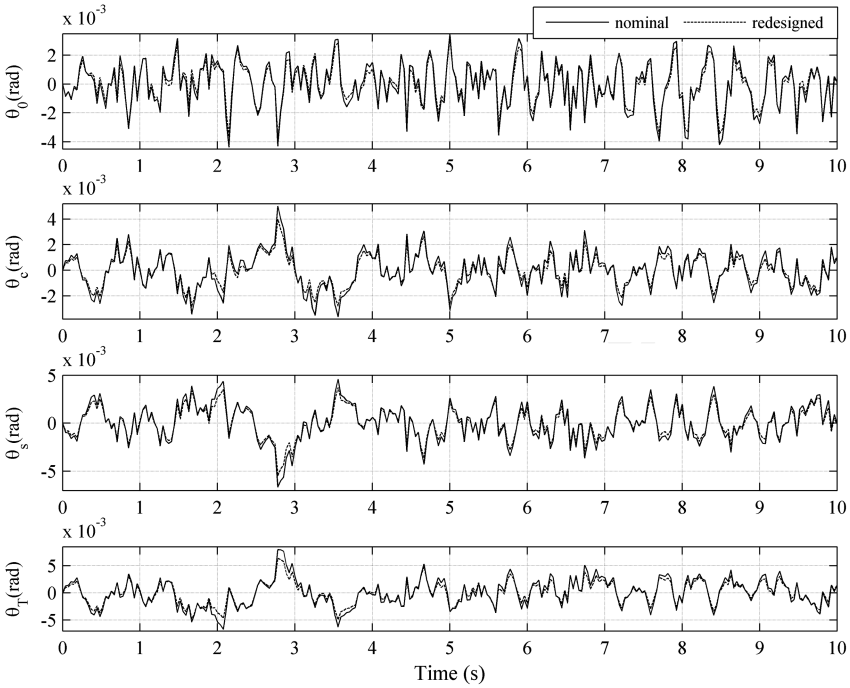

Fig. 9 Helicopter control responses before (nominal) and after redesign.

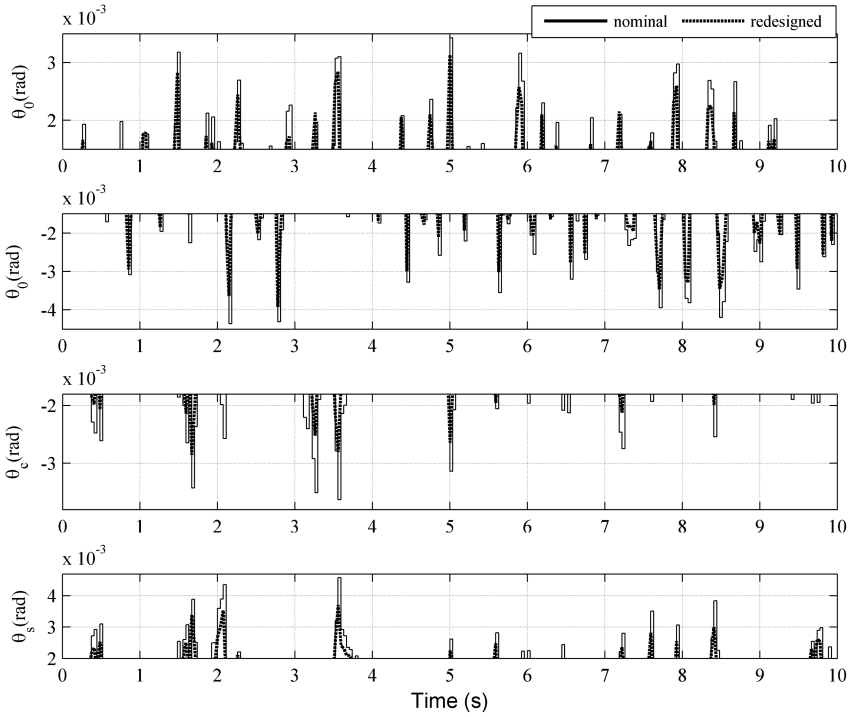

Fig. 10 Zoom for some helicopter control responses before (nominal) and after redesign.

To perform this study, we created two more closed-loop systems, referred to as the third and fourth closed-loop systems and defined as follows. First, we designed the OVC controller for the redesigned helicopter linearized around $V_A = 40$ kts (straight level flight). Then, we used this controller on the redesigned helicopter, which experiences 25% reduction in all helicopter inertial quantities, and it is linearized around a different flight condition, namely a helical turn characterized by $V_A = 80$ kts, $\gamma_{\mathrm{FP}} = 0.1$ rad, and $\dot{\psi}_A = 0.1$ rad/s. We thus obtained the third closed-loop system. Note that this is a challenging scenario for the controller because it operates on a system that experiences modeling uncertainties (i.e., inertial parameters variations) as well as qualitative and quantitative changes from the flight condition the controller was designed for (i.e., from straight level flight at $V_A = 40$ kts to helical turn at $V_A = 80$ kts). This situation corresponds to using an "unaware controller" because there is no information (provided, for example, by a supervisory control system) about changes in the flight condition, which would enable switching to a more appropriate controller. On the other hand, if information is available about a substantial change in the flight condition, switching between controllers can be performed. We refer to this latter situation as one in which "aware controllers" are used. This actually corresponds to the fourth closed-loop system described next.

For the fourth closed-loop system, we first designed the OVC for the redesigned helicopter, this time linearized around the helical turn characterized by $V_A = 80$ kts, $\gamma_{\mathrm{FP}} = 0.1$ rad, and $\dot{\psi}_A = 0.1$ rad/s. Then, we used this controller on the redesigned helicopter, which experiences 25% reduction in all helicopter inertial quantities and is linearized around the same helical turn (i.e., with $V_A = 80$ kts, $\gamma_{\mathrm{FP}} = 0.1$ rad, and $\dot{\psi}_A = 0.1$ rad/s). As noted previously, this situation is encountered when a supervisory decision system exists that ensures that, for certain maneuvers, appropriate controllers are used (i.e., aware controllers). In this scenario, the controller has to mitigate only inertial parameters variations.

Closed-loop responses of some helicopter Euler angles (i.e., ϕ_A and θ_A), longitudinal linear velocity (i.e., u), and lateral angular velocity (i.e., q) are given in Fig. 11. Closed-loop responses of collective and longitudinal flapping and lagging angles (i.e., β_0, β_c, ζ_0, and ζ_c) are given in Fig. 12. Closed-loop responses of all controls (i.e., θ_0, θ_c, θ_s, and θ_T) are given in Fig. 13. For all of these responses, the third and fourth closed-loop systems are both excited by white noise perturbations. In Figs. 11 and 12, the solid line shows the responses of some states obtained using the third closed-loop system, while the dotted line illustrates the responses of some states obtained using the fourth closed-loop system. In Fig. 13, the solid line shows the responses of controls obtained using the third closed-loop system, while the dotted line illustrates the responses of controls obtained using the fourth closed loop.

From Fig. 11, it can be easily seen that helicopter Euler angles (e.g., ϕ_A and θ_A) do not experience fast and large variations regardless of the type of controller used (i.e., aware or unaware OVC). Because for the fourth closed-loop system (i.e., solid line), aware OVC is used, the variances of outputs of interest (i.e., helicopter Euler angles) satisfy the constraints in Eq. (5), and this explains the good behavior observed. Because for the third closed-loop system (i.e., solid line), unaware OVC is used, the variances of outputs of interest (i.e., helicopter Euler angles) do not satisfy the constraints in Eq. (5). However, from simulations, it can be easily seen that, even in this situation, helicopter Euler angles (e.g., ϕ_A and θ_A) do not experience fast and large variations. This result and our extensive simulations (see [10] for other examples) indicate that OVCs have good robustness properties with respect to significant modeling uncertainties (i.e., flight conditions and helicopter inertial parameters variations).

From Fig. 11, it can also be seen that peak values of helicopter Euler angles (e.g., ϕ_A and θ_A) obtained using the fourth closed-loop system are smaller than the ones obtained using the third closed-loop system, emphasizing the advantage of using aware controllers. Note that similar results and conclusions are also valid for helicopter yaw angle response [10]. From Fig. 11, it can be also concluded that linear and angular velocities (e.g., u and q) do not experience catastrophic behavior regardless of the fact that we use aware or unaware OVCs.

From Fig. 12, it can be concluded that other key helicopter states (e.g., β_0, β_c, ζ_0, ζ_c) do not experience catastrophic behavior regardless of the fact that we use aware or unaware OVCs. In terms of control responses, from Fig. 13, it can be concluded that all helicopter controls (i.e., θ_0, θ_c, θ_s, and θ_T) do not experience fast and large variations regardless of the type of controller used (i.e., aware or unaware). This result is expected for the fourth closed-loop system because aware OVC is used for this example. Moreover, from Fig. 13, it can also be easily seen that helicopter controls show good behavior for the third closed-loop system. This result indicates that OVCs also

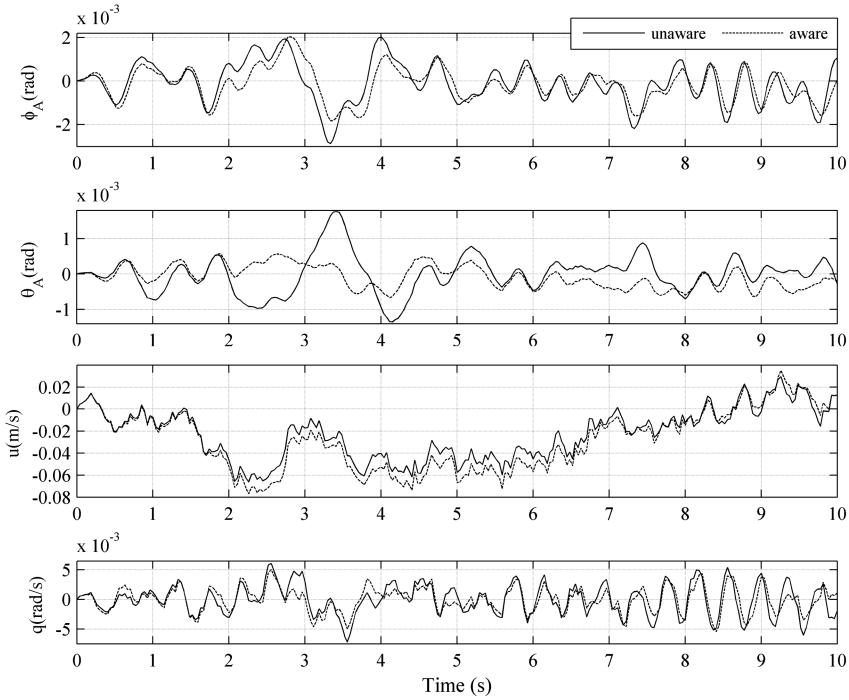

Fig. 11 Some fuselage state responses for robustness study.

have good robustness in terms of control responses. However, the peak values of most helicopter controls (i.e., θ_0, θ_c, and θ_T) obtained using the fourth closed-loop system are smaller than the ones obtained using the third closed-loop system. This is also another major advantage of using aware controllers.

E. Comprehensive Evaluation of the Redesign Process

To further investigate the efficiency of our simultaneous helicopter and control-system design procedure, we modified the lower and upper bounds on optimization parameters from $\pm 5\%$ to $\pm 10\%$ variations from their nominal values. Then, we followed the same steps given in Sec. V.A. The algorithm from Sec. IV.B was again very effective in rapidly decreasing the value of the objective J in the first several iterations (i.e., two iterations). Table 3 summarizes the new lower and upper bounds on optimization parameters as well as nominal and optimum values. The control energy corresponding to the redesigned system thus obtained was 56.8% lower than the control energy of the nominal system. Thus, we reach the same conclusion like before: small changes in some helicopter parameters may result in large savings in control energy if simultaneous helicopter and control-system design is performed.

To comprehensively evaluate the redesigned helicopter, we followed the same steps given in Sec. V.C. In Fig. 14, closed-loop responses of some helicopter Euler angles (i.e., ϕ_A and θ_A), longitudinal linear velocity (i.e., u), lateral angular velocity (i.e., q), collective blade flapping angle (i.e., β_0), and collective and lateral cyclic main-rotor controls (i.e., θ_0 and θ_s) are given when the fifth closed-loop system, the one obtained using nominal helicopter and

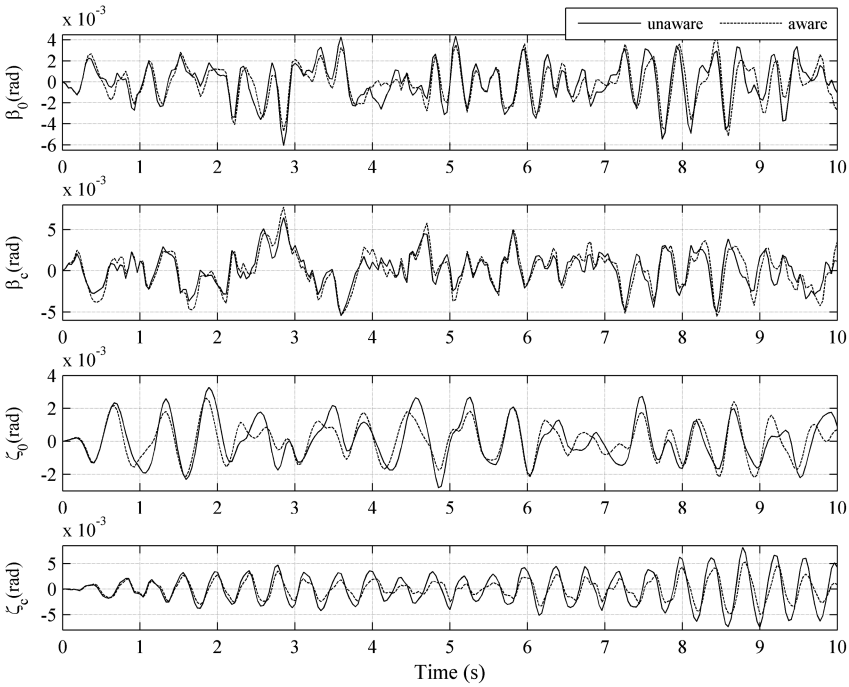

Fig. 12 Some blade state responses for robustness study.

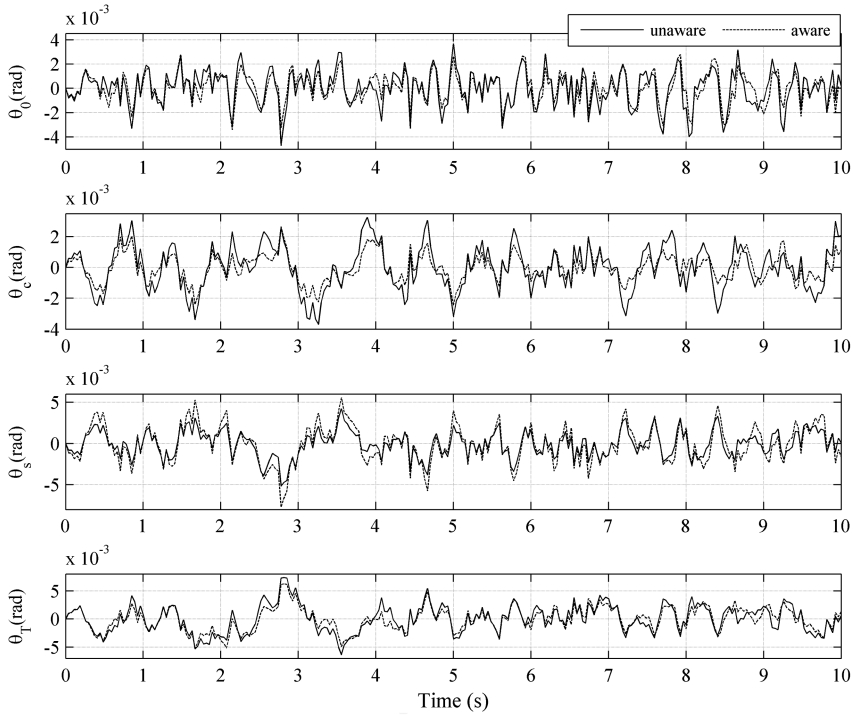

Fig. 13 Helicopter control responses for robustness study.

OVC designed for it (solid line), and sixth closed-loop system, obtained using new redesigned helicopter and OVC designed for it (dotted line), are both excited by white noise perturbations.

From Fig. 14, it can be ascertained that the conclusion regarding closed-loop response results found using the first redesigned helicopter (i.e., the one obtained in Sec. V.A) and the nominal helicopter (see Sec. V.C) are still valid for the closed-loop responses obtained using the new redesigned helicopter (i.e., the one obtained using the values in Table 3). For example, the qualitative and quantitative behaviors of helicopter Euler angles are the same before and after redesign, and the variances of outputs of interest (i.e., helicopter Euler angles) are very close and satisfy constraints [Eq. (5)]. Likewise, fuselage states and blade states do not experience catastrophic behavior before and after redesign (their qualitative behavior being similar), and the controls variations (e.g., θ_0 and θ_s) from their trim values decrease after redesign. In Fig. 15, comparison of peak values of some controls between first redesigned helicopter (i.e., the one obtained using the constraints in Table 2) and second redesigned helicopter (i.e., the one obtained using the constraints in Table 3) is illustrated. From Fig. 15, it can be again concluded that our simultaneous helicopter and control-system design idea is very useful for control energy saving.

We also evaluated robustness of the new redesigned helicopter using the same steps as in Sec. V.D. Closed-loop responses of some helicopter Euler angles (i.e., ϕ_A and θ_A), longitudinal linear velocity (i.e., u), lateral angular velocity (i.e., q), collective blade flapping angle (i.e., β_0), and collective and lateral cyclic main-rotor controls (i.e., θ_0 and θ_s) are given in Fig. 16. In Fig. 16, the solid line shows the responses of some states and controls obtained using the seventh closed-loop system, created using the unaware OVC and the new redesigned helicopter, while the dotted line illustrates the responses of controls obtained using the eighth closed-loop, created using the aware OVC and the new redesigned helicopter.

From Fig. 16, it can be concluded that the observations regarding robustness results found using the first redesigned helicopter (see Sec. V.D) are still valid for the robustness of the new redesigned helicopter. For example, any helicopter state (e.g., ϕ_A, θ_A, u, q, and β_0) does not experience catastrophic behavior regardless of the fact that we use aware or unaware OVCs. The peak values of helicopter Euler angles (e.g., ϕ_A and θ_A) obtained using the sixth closed-loop system are smaller than the ones obtained using the fifth closed-loop system. Helicopter controls (e.g., θ_0 and θ_s) do not experience fast and large variations regardless of the type of controller used (i.e., aware or unaware).

F. Maneuvering-Flight Results

We also investigated the efficiency of the simultaneous helicopter and control-system design using maneuvering-flight conditions, specifically level banked turn and helical turn. For this purpose, we linearized our model around $V_A = 40$ kts, $\gamma_{\mathrm{FP}} = 0$ rad, and $\dot{\psi}_A = 0.1$ rad/s (level banked turn). Then, we followed the same steps given in Sec. V.A, allowing $\pm 10\%$ variation in helicopter parameters for this new redesigned helicopter. The results are summarized in Table 4. The control energy corresponding to the redesigned system thus obtained was 57.0% lower than the control energy of the nominal system. The algorithm (see Sec. IV.B) is still very effective in rapidly decreasing the value of the objective, J, for level banked turn. Then, to comprehensively evaluate the new redesigned helicopter, we followed the same steps given in Sec. V.C.

In Fig. 17, closed-loop responses of some helicopter Euler angles (i.e., ϕ_A and θ_A), and collective and lateral cyclic main-rotor controls

Table 3 Design variables, nominal values, new constraints, and new optimum values

Design variable	Nominal value	Lower bound $\Delta x_i/x_i$	Upper bound $\Delta x_i/x_i$	New optimum value	Change $\Delta x_i/x_i$
c	0.5401 m	−0.1	0.1	0.5941 m	0.09998
K_β	48, 149 N · m/rad	−0.1	0.1	52, 483.5565 N · m/rad	0.09002
m	9.1 kg/m	−0.1	0.1	10.0098 kg/m	0.09998
R	7.5 m	−0.1	0.1	6.7536 m	−0.09952
θ_{tw}	−0.14 rad	−0.1	0.1	−0.1540 rad	−0.09976
Ω	27 rad/s	−0.1	0.1	24.3 rad/s	−0.09999

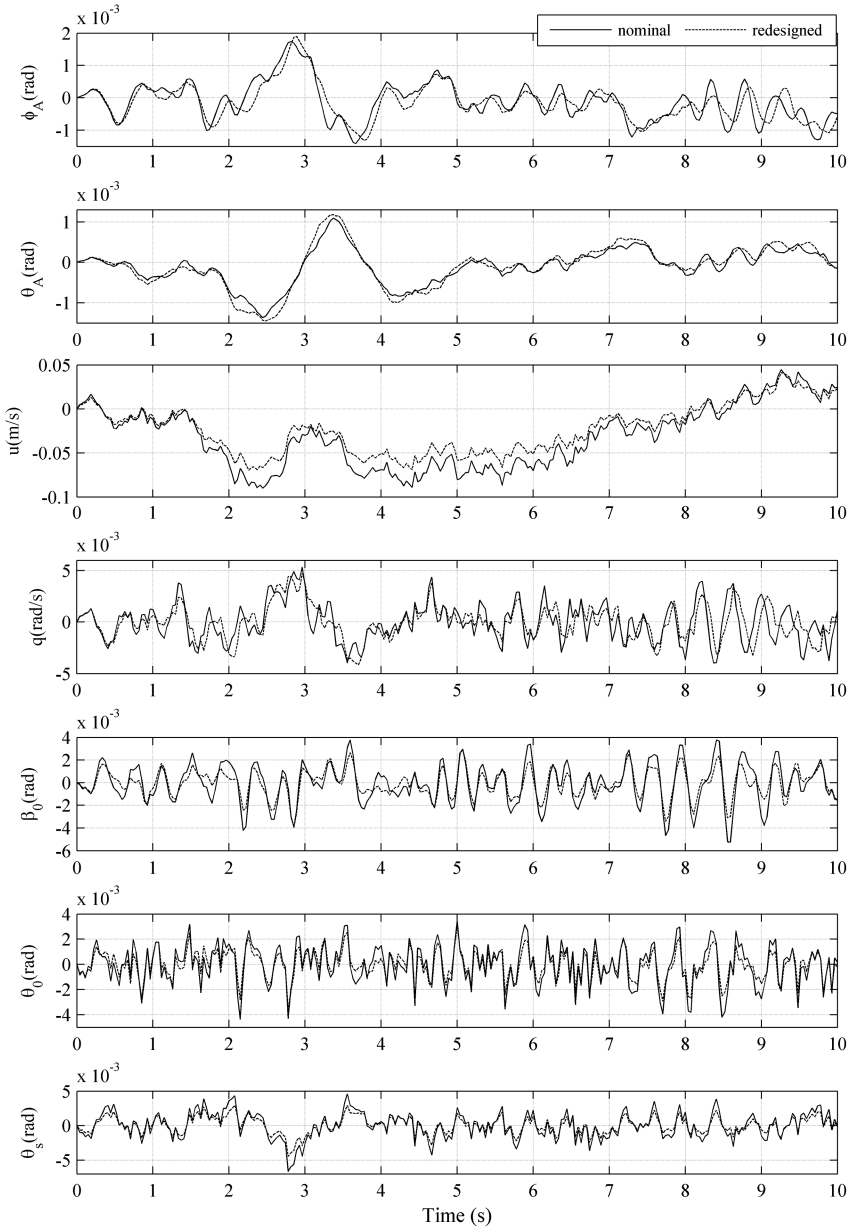

Fig. 14 Some helicopter state and control responses before (nominal) and after redesign (comprehensive evaluation).

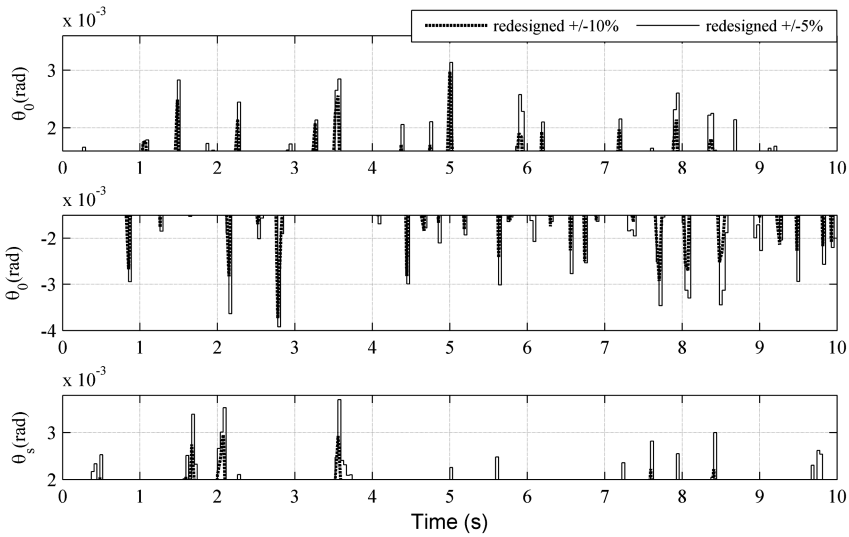

Fig. 15 Zoom for some helicopter control responses after two redesigns.

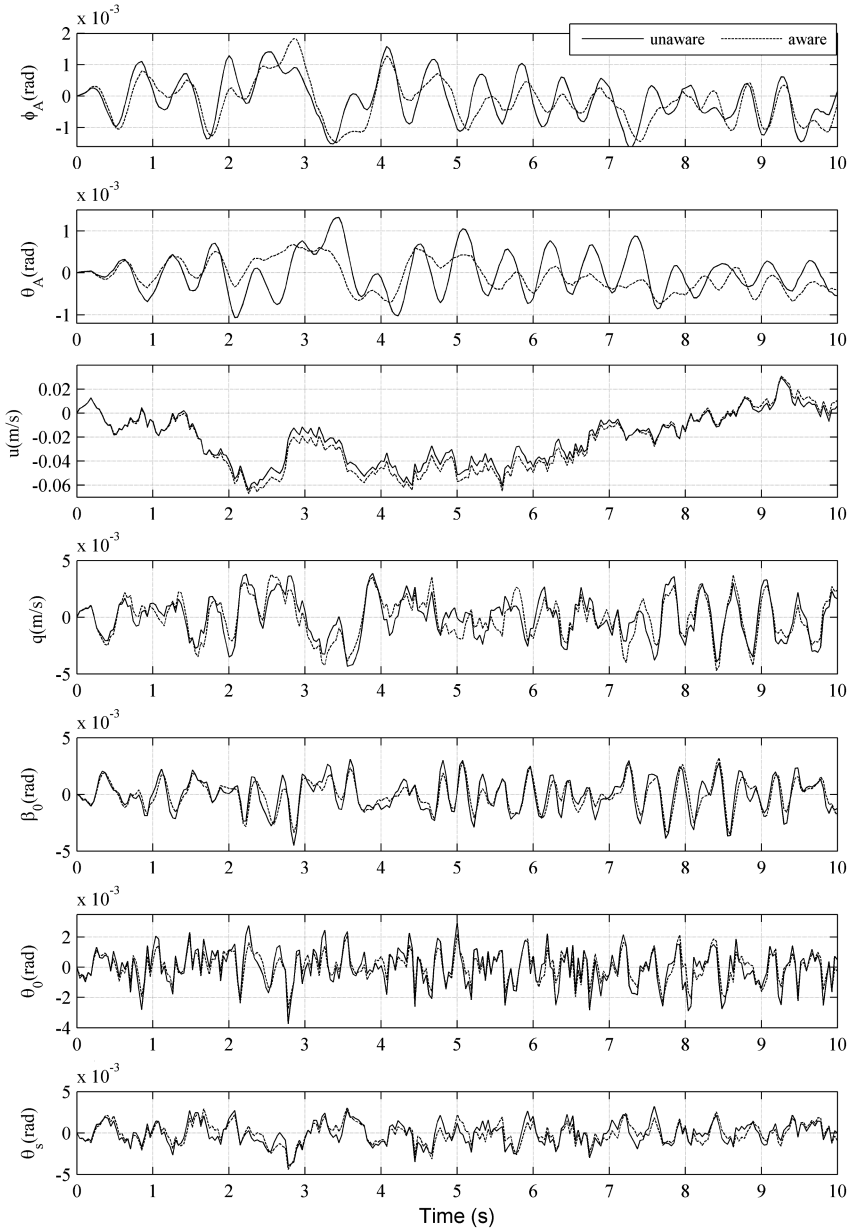

Fig. 16 Some helicopter state and control responses for robustness study (comprehensive evaluation).

(i.e., θ_0 and θ_s) are given when the ninth closed-loop system (i.e., the one created using maneuvering nominal helicopter and OVC designed for it, solid line) and the tenth closed-loop system (i.e., the one created using maneuvering redesigned helicopter and OVC designed for it, dotted line) are both excited by white noise perturbations.

Figure 17 and our extensive analysis show that the observations about the closed-loop responses reached using previous redesigned helicopters (see Secs. V.C and V.E) are still valid for the closed-loop responses obtained in this section. For example, the qualitative and quantitative behaviors of helicopter Euler angles are the same before and after redesign, and the variances of outputs of interest (i.e., helicopter Euler angles) are very close and satisfy constraints [Eq. (5)]. The controls variations (e.g., θ_0 and θ_s) from their trim values decrease after redesign. This reduction can be seen better in Fig. 18.

We also evaluated robustness of the redesigned helicopter obtained in this section, using the same steps as in Sec. V.D. Closed-loop responses of some helicopter Euler angles (i.e., ϕ_A and θ_A), and collective and lateral cyclic main-rotor controls (i.e., θ_0 and θ_s) are

Table 4 Design variables, nominal values, constraints, and optimum values (level banked turn, $V_A = 40$ kts, $\gamma_{FP} = 0$ rad, and $\dot{\psi}_A =$ rad/s

Design variable	Nominal value	Lower bound$\Delta x_i/x_i$	Upper bound$\Delta x_i/x_i$	New optimum value	Change$\Delta x_i/x_i$
c	0.5401 m	−0.1	0.1	0.5941 m	0.09998
K_β	48, 149 N · m/rad	−0.1	0.1	52, 940.7885 N · m/rad	0.09952
m	9.1 kg/m	−0.1	0.1	10.0098 kg/m	0.09998
R	7.5 m	−0.1	0.1	6.7501 m	−0.09999
θ_{tw}	−0.14 rad	−0.1	0.1	−0.1260 rad	−0.09998
Ω	27 rad/s	−0.1	0.1	24.3 rad/s	−0.09999

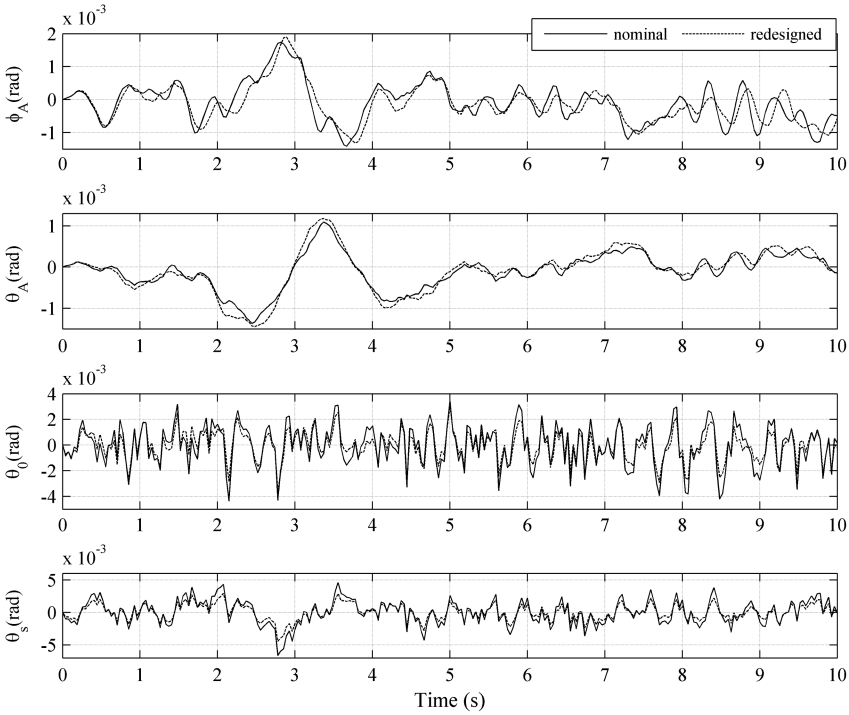

Fig. 17 Some helicopter state and control responses before (nominal) and after redesign during maneuvering flight.

given in Fig. 19. In Fig. 19, the solid line shows the responses of some states and controls obtained using the 11th closed-loop system (i.e., the one created using the unaware OVC and the redesigned helicopter obtained using a level banked turn design point), while dotted line illustrates the responses of controls obtained using the 12th closed loop (i.e., the one created using the aware OVC and the redesigned helicopter obtained using a level banked turn design point).

From Fig. 19, it can be ascertained that the robustness conclusions found using previous redesigned helicopters (see Secs. V.D and V.E) are still valid for the robustness of this redesigned helicopter. For example, the peak values of helicopter Euler angles (e.g., ϕ_A and θ_A) obtained using the 12th closed-loop system are smaller than the ones obtained using the 11th closed-loop system, and helicopter controls (e.g., θ_0 and θ_s) do not experience fast and large variations regardless of the type of controller used (i.e., aware or unaware). We also linearized our model around $V_A = 40$ kts, $\gamma_{\mathrm{FP}} = 0.1$ rad, and $\dot{\psi}_A = 0.1$ rad/s (helical turn) and then followed the same steps in this section and reached very similar conclusions.

An important observation regarding the practical implementation of these results is necessary. Our approach is to simultaneously design the helicopter and the controller using models linearized around different operational conditions. A natural question is, "How would one implement this idea when operational conditions change?" The answer is provided by recent technological advances in the area of morphing helicopter that inspired our work, for example [3–5,20–26]. These advances enable changes in the helicopter parameters that we use for design in our paper: blade length, chord length, flapping-spring stiffness, twist, linear mass density, and main-rotor angular speed. Therefore, when the operational conditions change, helicopter parameters can be modified from optimal values corresponding to one operational condition to optimal values corresponding to another operational condition. In parallel, the controller will also change from one optimal controller to another. It is clear that this scenario corresponds to the gain scheduling idea that is so popular in control design. Therefore, for implementation of our idea, we schedule both the controller gains and the helicopter parameters to achieve optimal flying conditions across a wide flight envelope.

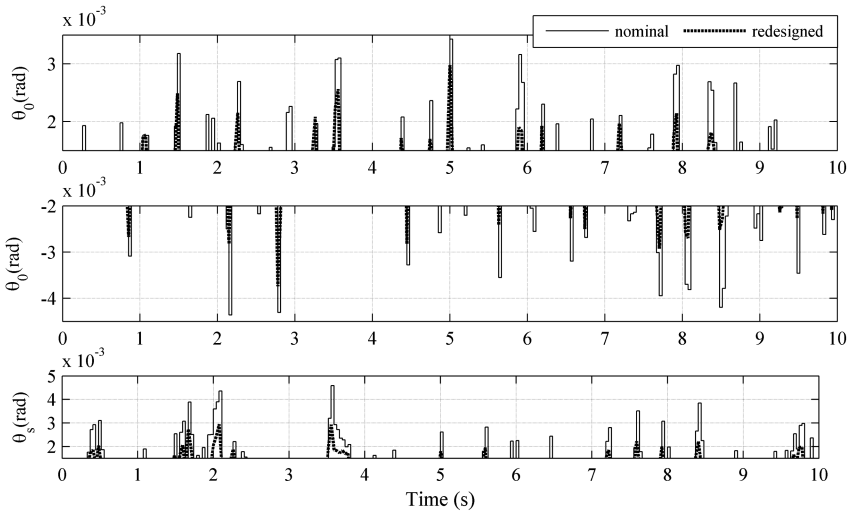

Fig. 18 Zoom for some control responses before (nominal) and after redesign during maneuvering flight.

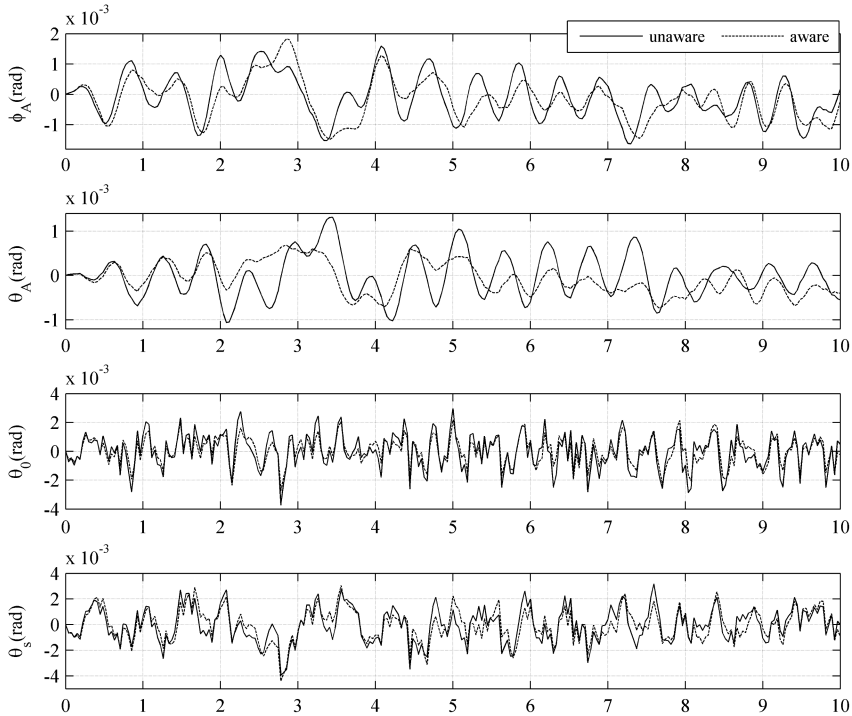

Fig. 19 Some helicopter state and control responses during maneuvering flight for robustness study.

Table A1 Scenarios

SPSA number	Design point	Allowable change	Evaluated	Section
First SPSA	40 kt straight level flight	±5%%	40 kt straight level flight	Secs. V.A, V.B, V.C
First SPSA	40 kt straight level flight	±5%	80 kt helical turn	Sec. V.D
Second SPSA	40 kt straight level flight	±10%	40 kt straight level flight	Sec. V.E
Second SPSA	40 kt straight level flight	±10%	80 kt helical turn	Sec. V.E
Third SPSA	40 kt level banked turn	±10%	40 kt level banked turn	Sec. V.F
Third SPSA	40 kt level banked turn	±10%	80 kt helical turn	Sec. V.F

VI. Conclusions

Simultaneous helicopter and control-system design is investigated to save control energy while output variance constraints are also satisfied. Complex, control-oriented, physics-based helicopter models are used for this purpose. An optimization algorithm that solves the simultaneous design problem using a novel modified stochastic optimization method is developed and illustrated on straight level flights, level banked turns, and helical turns.

The aforementioned optimization algorithm is very effective in rapidly decreasing the control energy. Considerable reduction of control energy (i.e., around 30% for ±5% parameter variation and around 55% for ±10% parameter variation) is obtained via simultaneous design compared to the situation when a sequential design approach (i.e., helicopter design followed by control-system design) is used. Moreover, this substantial control energy reduction is obtained using very small (i.e., ±5% and ±10%) changes in some helicopter parameters such as blade length, blade chord length, blade flapping-spring stiffness, blade twist, blade linear mass density, and main-rotor angular speed. Such small changes are easily achievable and nowadays technologically feasible. It should be emphasized that the energy savings reported herein are obtained using linearized helicopter models. In practical applications, because of inherent helicopter nonlinearities, the real energy savings can be slightly different from values computed using linearized models.

Furthermore, the qualitative behaviors of fuselage and blade states before (i.e., when the sequential design approach is used) and after redesign (i.e., when the simultaneous design approach is used) are similar, and they do not display dangerous behaviors such as very large amplitudes and fast oscillations. The outputs of interest (i.e., helicopter Euler angles) before and after redesign also display qualitatively and quantitatively similar behaviors, while satisfying all of the variance constraints. The peak values of helicopter controls decrease after redesign, which explains the considerable reduction of control energy observed when simultaneous helicopter and control-system design is performed.

Last, our extensive analysis indicated that output variance-constrained controllers, which are designed for the redesigned helicopter, have very good robustness properties with respect to variations in flight conditions as well as helicopter inertial properties.

References

[1] Grigoriadis, K. M., Carpenter, M. J., Zhu, G., and Skelton, R. E., "Optimal Redesign of Linear Systems," *Proceedings of the American Control Conference*, San Francisco, CA, 1993.

[2] Grigoriadis, K. M., Zhu, G., and Skelton, R. E., "Optimal Redesign of Linear Systems," *Journal of Dynamic Systems, Measurement and Control*, Vol. 118, No. 3, 1996, pp. 598–605. doi: 10.1115/1.2801186

[3] Guo, W., and Horn, J. F., "Rotor State Feedback Control for Rotorcraft with Variable Rotor Speed," *AIAA Guidance, Navigation, and Control Conference*, AIAA Paper 2009-5797, 2009.

[4] Horn, J. F., Guo, W., and Ozdemir, G. H., "Use of Rotor State Feedback to Improve Closed-Loop Stability and Handling Qualities," *Journal of the American Helicopter Society*, Vol. 7, No. 2, April 2012, pp. 1–10. doi:10.4050/JAHS.57.022001

[5] Kang, H., Saberi, H., and Gandhi, F., "Dynamic Blade Shape for Improved Helicopter Rotor Performance," *Journal of the American Helicopter Society*, Vol. 55, No. 3, 2010, pp. 32008-1–32008-11. doi:10.4050/JAHS.55.032008

[6] Fusato, D., and Celi, R., "Multidisciplinary Design Optimization for Helicopter Aeromechanics and Handling Qualities," *Journal of Aircraft*,

Vol. 43, No. 1, 2006, pp. 241–252.
doi:10.2514/1.7943

[7] Ganguli, R., "Optimum Design of a Helicopter Rotor for Low Vibration Using Aeroelastic Analysis and Response Surface Methods," *Journal of Sound and Vibration*, Vol. 258, No. 2, 2002, pp. 327–344.
doi:10.1006/jsvi.2002.5179

[8] Celi, R., "Recent Applications of Design Optimization to Rotorcraft—A Survey," *Journal of Aircraft*, Vol. 36, No. 1, 1999, pp. 176–189.
doi:10.2514/2.2424

[9] Friedmann, P. P., "Helicopter Vibration Reduction Using Structural Optimization with Aeroelastic/Multidisciplinary Constraints—A Survey," *Journal of Aircraft*, Vol. 28, No. 1, 1991, pp. 8–21.
doi:10.2514/3.45987

[10] Oktay, T., "Constrained Control of Complex Helicopter Models," Ph.D. Dissertation, Virginia Polytechnic Inst. and State Univ., Blacksburg, VA, May 2012.

[11] Skelton, R. E., *Dynamic Systems Control: Linear Systems Analysis and Synthesis*, John Wiley & Sons, 1987, pp. 329–397, Chap. 8.

[12] Skelton, R. E., Iwasaki, T., and Grigoriadis, K. M., *A Unified Algebraic Approach to Linear Control Design*, Taylor and Francis, 1998, pp. 121–199, Chap. 4.

[13] Skelton, R. E., and Lorenzo, M. D., "Space Structure Control Design by Variance Assignment," *Journal of Guidance, Control, and Dynamics*, Vol. 8, No. 4, 1985, pp. 454–462.
doi:10.2514/3.20005

[14] Hsieh, C., Skelton, R. E., and Damra, F. M., "Minimum Energy Controllers with Inequality Constraints on Output Variances," *Optimal Control Application and Methods*, Vol. 10, No. 4, 1989, pp. 347–366.
doi:10.1002/oca.4660100405

[15] Zhu, G., and Skelton, R. E., "Mixed L_2 and L_∞ Problems by Weight Selection in Quadratic Optimal Control," *International Journal of Quadratic Optimal Control*, Vol. 63, No. 5, 1991, pp. 1161–1176.
doi:10.1080/00207179108953668

[16] Zhu, G., Rotea, M. A., and Skelton, R. E., "A Convergent Algorithm for the Output Covariance Constraint Control Problem," *SIAM Journal on Control and Optimization*, Vol. 35, No. 1, 1997, pp. 341–361.
doi:10.1137/S0363012994263974

[17] Skelton, R. E., and Sultan, C., "Controllable Tensegrity, a New Class of Smart structures," *SPIE International Symposium on Smart Structures and Materials*, SPIE, Belligham, WA, 1997, pp. 166–177.

[18] Sultan, C., and Skelton, R. E., "Integrated Design of Controllable Tensegrity Structures," *ASME International Mechanical Engineering Congress and Exposition*, ASME, New York, 1997, pp. 27–37.

[19] Oktay, T., and Sultan, C., "Variance Constrained Control of Maneuvering Helicopters," *Proceedings of the American Helicopter Society 68th Forum*, Forth Worth, TX, May 2012.

[20] Wilbur, M., and Sekula, M., "The Effect of Tip Geometry on Active Twist Rotor Response," *Proceedings of the American Helicopter Society 61st Annual Forum*, Grapevine, TX, 2005.

[21] Yeo, H., "Assessment of Active Controls for Rotor Performance Enhancement," *Journal of the American Helicopter Society*, Vol. 53, No. 2, 2008, pp. 152–163.
doi:10.4050/JAHS.53.152

[22] Asar, M., Ray, A., and Horn, J. F., "A Comprehensive Control Strategy for Integrated Flight/Propulsion Systems," *Proceedings of the Institute of Mechanical Engineers, Part G Journal of Aerospace Engineering*, Vol. 222, No. 6, 2008, pp. 843–859.
doi:10.1243/09544100JAERO297

[23] Kang, H., Saberi, H., and Gandhi, F., "Dynamic Blade Shape for Improved Helicopter Rotor Performance," *Journal of the American Helicopter Society*, Vol. 55, No. 3, 2010, p. 32008.
doi:10.4050/JAHS.55.032008

[24] Khoshlahjeh, M., Barbarino, S., Gandhi, F., and Webster, S., "Helicopter Performance Improvement with Variable Chord Morphing Rotors," *Proceedings of the 36th European Rotorcraft Forum*, Paris, 2010.

[25] Khoshlahjeh, M., Gandhi, F., and Webster, S., "Extendable Chord Rotors for Helicopter Envelope Expansion and Performance Improvement," *Proceedings of the 67th American Helicopter Society Annual Forum*, Virginia Beach, VA, 2011.

[26] Barbarino, S., Gandhi, F., and Webster, S., "Design of Extendable Chord Sections for Morphing Helicopter Rotor Blades," *Journal of Intelligent Material Systems and Structures*, Vol. 22, No. 9, 2011, pp. 365–378.
doi:10.1177/1045389X11414077

[27] Spall, J. C., "Multivariable Stochastic Approximation Using a Simultaneous Perturbation Gradient Approximation," *IEEE Transactions on Automatic Control*, Vol. 37, No. 3, 1992, pp. 332–341.
doi:10.1109/9.119632

[28] Sultan, C., "Proportional Damping Approximation Using the Energy Gain and Simultaneous Perturbation Stochastic Approximation," *Mechanical Systems and Signal Processing*, Vol. 24, No. 7, 2010, pp. 2210–2224.
doi:10.1016/j.ymssp.2010.02.013

[29] Oktay, T., and Sultan, C., "Integrated Maneuvering Helicopter Model and Controller Design," *Proceedings of AIAA Guidance, Navigation, and Control Conference*, AIAA Paper 2012-4596, Aug. 2012.

[30] Oktay, T., and Sultan, C., "Model Predictive Control of Maneuvering Helicopters," *Proceedings of AIAA Guidance, Navigation, and Control Conference*, AIAA Paper 2012-4530, Aug. 2012.

[31] Padfield, G. D., *Helicopter Flight Dynamics*, AIAA Education Series, AIAA, Reston, VA, 2007, pp. 265–267.

[32] He, Y., Fu, M. C., and Marcus, S. I., "Convergence of Simultaneous Perturbation Stochastic Approximation for Non-Differentiable Optimization," *IEEE Transactions on Aerospace and Electronic Systems*, Vol. 48, No. 8, 2003, pp. 1459–1463.
doi:10.1109/TAC.2003.815008

[33] Maryak, J. L., and Chin, D. C., "Global Random Optimization by Simultaneous Perturbation Stochastic Approximation," *Proceedings of the American Control Conference*, Arlington, VA, 2001.

[34] Wang, I. J., and Spall, J. C., "Stochastic Optimization with Inequality Constraints Using Simultaneous Perturbations and Penalty Functions," *Proceedings of the Conference on Decision and Control*, Maui, HI, 2003.

[35] Sadegh, P., and Spall, J. C., "Optimal Random Perturbations for Multivariable Stochastic Approximation Using a Simultaneous Perturbation Gradient Approximation," *IEEE Transactions on Automatic Control*, Vol. 43, No. 10, 1998, pp. 1480–1484.
doi:10.1109/9.720513

[36] Spall, J. C., "Implementation of the Simultaneous Perturbation Algorithm for Stochastic Optimization," *IEEE Transactions on Aerospace and Electronic Systems*, Vol. 34, No. 3, 1998, pp. 817–823.
doi:10.1109/7.705889

[37] Fabian, V., "Stochastic Approximation," *Optimizing Methods in Statistics*, edited by Rustigi, J. J., Academic Press, New York, 1971, pp. 439–470.

[38] Chin, D. C., "Comparative Study of Stochastic Algorithms for System Optimization Based on Gradient Approximation," *IEEE Transactions on Systems, Man, and Cybernetics*, Vol. 27, No. 2, 1997, pp. 244–249.
doi:10.1109/3477.558808